Coherence Properties of Individual Femtosecond Pulses of an X-Ray Free-Electron Laser

I. A. Vartanyants,[1,2,*] A. Singer,[1] A. P. Mancuso,[1,†] O. M. Yefanov,[1] A. Sakdinawat,[3] Y. Liu,[3] E. Bang,[3] G. J. Williams,[4] G. Cadenazzi,[5] B. Abbey,[5] H. Sinn,[6] D. Attwood,[3] K. A. Nugent,[5] E. Weckert,[1] T. Wang,[4] D. Zhu,[4] B. Wu,[4] C. Graves,[4] A. Scherz,[4] J. J. Turner,[4] W. F. Schlotter,[4] M. Messerschmidt,[4] J. Lüning,[7] Y. Acremann,[8] P. Heimann,[9] D. C. Mancini,[10] V. Joshi,[10] J. Krzywinski,[4] R. Soufli,[11] M. Fernandez-Perea,[11] S. Hau-Riege,[11] A. G. Peele,[12] Y. Feng,[4] O. Krupin,[4,6] S. Moeller,[4] and W. Wurth[13]

[1]Deutsches Elektronen-Synchrotron DESY, Notkestrasse 85, D-22607 Hamburg, Germany
[2]National Research Nuclear University, "MEPhI," 115409 Moscow, Russia
[3]University of California, Berkeley, California 94720, USA
[4]SLAC National Accelerator Laboratory, 2575 Sand Hill Road, Menlo Park, California 94025-7015, USA
[5]ARC Centre of Excellence for Coherent X-ray Science, School of Physics, The University of Melbourne, Victoria, 3010, Australia
[6]European XFEL GmbH, Albert-Einstein-Ring 19, 22761 Hamburg, Germany
[7]Laboratoire de Chimie Physique - Matière et Rayonnement, UMR 7614 (CNRS), Université Pierre et Marie Curie, Paris, France
[8]ETH Zürich, Laboratorium für Festkörperphysik, Schafmattstrasse 16, 8093 Zürich, Switzerland
[9]Advanced Light Source, Lawrence Berkeley National Laboratory, Berkeley, California 94720, USA
[10]Advanced Photon Source and Center for Nanoscale Materials, Argonne National Laboratory, Argonne, Illinois 60439, USA
[11]Lawrence Livermore National Laboratory, 7000 East Avenue, Livermore, California 94550, USA
[12]ARC Centre of Excellence for Coherent X-ray Science Department of Physics, La Trobe University, Melbourne, Victoria 3086, Australian Synchrotron, Clayton, 3168 Australia
[13]Institut für Experimentalphysik and CFEL, University of Hamburg, Luruper Chaussee 149, 22761 Hamburg, Germany
(Received 16 May 2011; published 30 September 2011)

Measurements of the spatial and temporal coherence of single, femtosecond x-ray pulses generated by the first hard x-ray free-electron laser, the Linac Coherent Light Source, are presented. Single-shot measurements were performed at 780 eV x-ray photon energy using apertures containing double pinholes in ''diffract-and-destroy'' mode. We determined a coherence length of 17 μm in the vertical direction, which is approximately the size of the focused Linac Coherent Light Source beam in the same direction. The analysis of the diffraction patterns produced by the pinholes with the largest separation yields an estimate of the temporal coherence time of 0.55 fs. We find that the total degree of transverse coherence is 56% and that the x-ray pulses are adequately described by two transverse coherent modes in each direction. This leads us to the conclusion that 78% of the total power is contained in the dominant mode.

DOI: 10.1103/PhysRevLett.107.144801 PACS numbers: 41.60.Cr, 42.25.Hz, 42.25.Kb, 42.55.Vc

Coherence is the fundamental property of light waves produced by laser sources. In combination with ultrashort pulses, they yield insight into basic questions in physics through real-time observation and control of atomic scale structure and dynamics [1]. The recent development of x-ray free-electron lasers (XFELs) in the extreme ultraviolet [2] and the hard x-ray range [3–5] with their unprecedented peak brightness, short pulse duration—from 500 to 10 fs and below—and, importantly, a high degree of transverse coherence, opens new frontiers in the study of the structure and dynamics of matter.

The intense, coherent, and ultrashort x-ray pulses produced by XFELs promise important new insights in biology [6,7], condensed matter physics [8], and atomic physics [9]. They have already paved the way for new approaches to protein crystallography using nanocrystals [10] and the imaging of single viruses [11]. Spatial coherence is essential for applications such as coherent x-ray diffractive imaging [12–14], x-ray holography [15], and x-ray photon correlation spectroscopy [16]. The recovery of structural information from coherent imaging experiments relies on a high degree of spatial coherence in the incident field to enable the phasing of the diffraction pattern [17,18] produced by its scattering from the sample. Despite this importance, no direct measurements of the coherence properties of XFEL beams from hard x-ray FELs have been reported, although estimates of the coherence properties of these sources have been available through simulations [19,20]. Here we present measurements of the coherence of the Linac Coherent Light Source (LCLS) x-ray beam.

One of the most widely used methods for characterization of coherence is Young's experiment [21], where two small pinholes separated by a certain distance are illuminated. The visibility of the resultant interference pattern is a measure of the correlation within the wave field incident at the two pinholes—that is, the transverse coherence of the illuminating beam. An analysis of the contrast of these interference fringes, as a function of their distance from the center of the diffraction pattern, can also yield a measurement of the temporal coherence. This method has been successfully employed with light beams [22] and x rays at

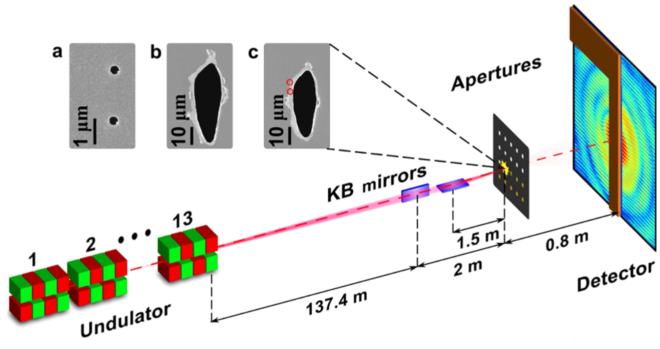

FIG. 1 (color online). A sketch of the experiment showing 13 undulator modules, a set of Kirkpatrick-Baez mirrors focusing the beam on a sample frame and the detector, protected from the direct beam by a beamstop. The inset shows scanning electron microscopy images of different apertures before (a) and after (b) the exposure of a single LCLS pulse. The inset (c) shows a case when the center of the beam missed the double pinhole (marked by the red circles).

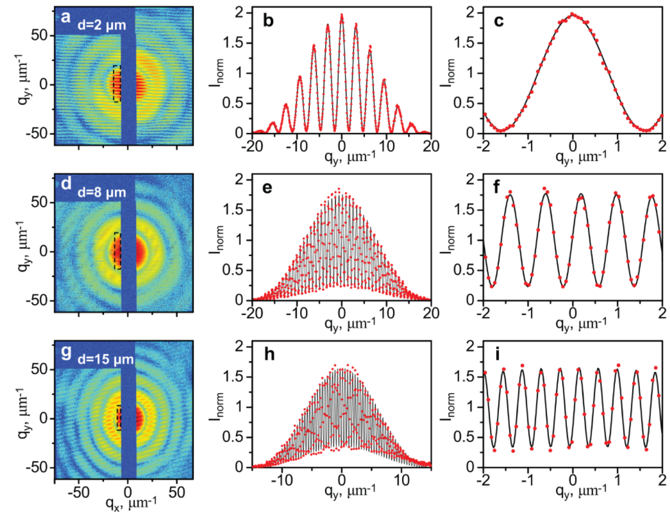

FIG. 2 (color online). Measured diffraction patterns. Left column: Interference fringes from pinholes separated by 2 (a), 8 (d), and 15 μm (g), each exposed to a single shot of the LCLS beam as a function of the transverse momentum transfer q_x, q_y. The area used for the analysis of the transverse coherence is shown by the dashed black rectangle close to the center of the patterns. Middle column: Line scans of the interference fringes on the right edge of the marked region, experimental data (red dots), and results of the theoretical fit (black lines). Right column: Enlarged regions of the line scans shown in the middle column.

synchrotrons [23] and in the extreme ultraviolet energy range also using pulsed sources [24–28].

The goal of this experiment is to characterize the coherence properties of individual, focused LCLS pulses using double pinhole apertures. These single-shot measurements were performed in the ‘‘diffract-and-destroy’’ mode [14].

The experiment was conducted at the soft x-ray research (SXR) instrument of the LCLS. A sketch of the experiment is shown in Fig. 1. The LCLS was operated with an electron bunch charge of 250 pC and with 13 undulator segments tuned to deliver 780 eV ($\lambda = 1.6$ nm) x-ray photons. Under these conditions, LCLS is expected to reach its saturation regime [3,20,29]. The duration of a single pulse was about 300 fs, determined from electron bunch measurements. The average energy was about 1 mJ per pulse. The beam was delivered to the end station through a beam transport system that includes three plane distribution mirrors and a monochromator comprised of a spherical mirror followed by a plane grating [30]. The measurements presented here were performed with the monochromator grating replaced by a plane mirror. The spherical mirror was operated in grazing incidence geometry (incidence angle of 89.2°) and focused the beam at the exit slit of the monochromator (focal length 7.8 m). The limiting vertical aperture of the beam delivery system was twice the full width at half maximum (FWHM) of the beam size at the grating position at 800 eV photon energy. At the sample position, the beam was focused to a size of 5.7 ± 0.4 μm (FWHM) in the horizontal and 17.3 ± 2.4 μm (FWHM) in the vertical direction [31] by a pair of bendable Kirkpatrick-Baez mirrors consisting of a silicon substrate coated with a 37.4 nm thick boron carbide reflective coating [32–34], with focal lengths of 1.5 (V) and 2 m (H).

A multiple aperture array [31] with varying pinhole separations in the range from 2 to 15 μm was positioned in the focus of the beam inside the resonant coherent imaging end station (Fig. 1). After each shot on the sample, the array was moved to an unexposed sample position. To accumulate statistics, each pinhole configuration was measured several times, giving 110 patterns in total. Interference patterns were recorded by a Princeton Instruments PI-MTE 2048B direct illumination charge-coupled device (CCD) with 2048×2048 pixels, each 13.5×13.5 μm^2 in size, positioned 80 cm downstream from the apertures (Fig. 1). A 3 mm wide rectangular beamstop manufactured from B_4C was positioned in front of the CCD to protect it from exposure to the direct FEL beam.

Figure 2 shows typical single-shot diffraction patterns measured with different pinhole separations. For small separations between the pinholes, a high contrast diffraction pattern was observed, implying a high degree of coherence on that length scale. For larger separations, the visibility of the fringes is slightly reduced due to the partial coherence of the incoming beam.

The interference pattern $I(P)$ observed in a double pinhole experiment at the point P of the detector for narrow-bandwidth radiation can be described by the following expression [21,22,35,36]:

$$I(P) = I_0(P)\{1 + |\gamma_{12}^{\mathrm{eff}}(\tau)| \cos[\omega\tau - \alpha_{12}(\tau)]\}, \quad (1)$$

where $I_0(P)$ is the Airy distribution due to diffraction through a round pinhole of diameter D [21], τ is the time delay for the radiation to reach point P from different pinholes, ω is a mean frequency of the incoming radiation, and $\alpha_{12}(\tau)$ is the relative phase. The modulus of the effective complex degree of coherence $|\gamma_{12}^{\rm eff}(\tau)|$ in Eq. (1) is defined as $|\gamma_{12}^{\rm eff}(\tau)| = 2[\sqrt{I_1 I_2}/(I_1 + I_2)]|\gamma_{12}(\tau)|$, where $\gamma_{12}(\tau)$ is the intrinsic complex degree of coherence and $I_{1,2}$ are intensities incident at the pinholes one and two. When the incident intensities at both pinholes are identical, $|\gamma_{12}^{\rm eff}(\tau)| = |\gamma_{12}(\tau)|$.

The analysis of the diffraction data was performed by fitting expression (1) to each measured diffraction pattern [31] (see Fig. 2). In this analysis, we considered a region of the diffraction pattern shown in Fig. 2, where $|\gamma_{12}^{\rm eff}(\tau)| \approx |\gamma_{12}^{\rm eff}(0)|$ and $\alpha_{12}(\tau) \approx \alpha_{12}(0)$ are good approximations as the time delay associated with the path-length difference in this region is much shorter than the coherence time τ_c: $\tau \ll \tau_c$ (see below). The modulus of the effective complex degree of coherence $|\gamma_{12}^{\rm eff}|$ at a particular pinhole separation was determined for each shot (Fig. 3). A Gaussian fit, $\exp(-d^2/2l_y^{c2})$, through the "best" shots (those that provided the highest degree of coherence and shown as black squares in Fig. 3) gives an upper estimate for the root-mean-square (rms) value of the transverse coherence length, $l_y^c = 16.8 \pm 1.7$ μm, of the focused LCLS beam in the vertical direction.

Our analysis shows a significant variation of the effective degree of coherence between different pulses for the same pinhole separation (see Fig. 3). While this variation could be explained by shot-to-shot fluctuations of the coherence properties of the XFEL beam, it may also arise from uncertainty in the position of the incoming beam with respect to the center of the pinhole pair, which leads to a difference in intensity at each pinhole. The value of the effective complex degree of coherence $|\gamma_{12}^{\rm eff}|$ can be significantly lower than the intrinsic complex degree of coherence $|\gamma_{12}|$ if these incident intensities are not equal. To determine the possible maximum deviation of the incident pulses with respect to the center of the pinhole pair, we observed that some pulses were not centered on the apertures and did not destroy the pinholes [see inset (c) in Fig. 1]. We analyzed scanning electron microscopy images of these apertures and determined a maximum deviation of 11 μm in the vertical direction. The impact of this positional uncertainty on the contrast, deduced from the beam size and the Gaussian fit through the best shots, is described by the blue dashed line in Fig. 3. Our data indicate that most of the experimentally determined values lie in the range between the two lines corresponding to the best and the maximum offset shots. From this we conclude that this positional uncertainty is the dominant cause of the apparent shot-to-shot variation of the complex degree of coherence (see Fig. 2 in Ref. [31]).

Some of the pulses (six in total) that illuminated apertures with larger pinhole separations (greater than 10 μm) were extremely bright. This allows the determination of the fringe visibility up to the edge of the detector, which corresponds to time delays of $\tau \approx 0.6$ fs. At these conditions the time dependence in Eq. (1) was taken into account explicitly, providing a measurement of the temporal coherence for individual femtosecond pulses. For each selected pulse the visibility $|\gamma_{12}^{\rm eff}(\tau)|$ as a function of τ was fit by a Gaussian, $\exp(-\tau^2/2\tau_c^2)$. An average $\bar{\tau}_c$ of the determined values of τ_c yields a temporal coherence time $\bar{\tau}_c \approx 0.55 \pm 0.12$ fs (rms). For a beam with a Gaussian spectrum, this value is in good agreement with the estimate [21] $\tau_c \sim 1/\sigma_\omega = 0.4$ fs, where $\sigma_\omega = 2.5$ fs^{-1} is the rms bandwidth of the LCLS beam at that energy [29].

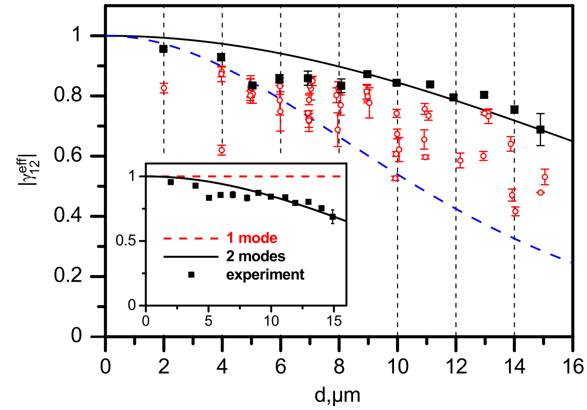

FIG. 3 (color online). The modulus of the effective complex degree of coherence $|\gamma_{12}^{\rm eff}|$ as a function of pinhole separation. The experimental values determined from the fitting procedure are shown by red circles. The error bars show the standard deviation of these values. A Gaussian function (black line) has been fit to the best shot values (black squares) which gives a coherence length of 16.8 ± 1.7 μm. The blue dashed line shows the decrease in the value of $|\gamma_{12}^{\rm eff}|$ due to the maximum measured offset between the position of the apertures and the incident beam. (Inset) The contribution of higher order modes to the modulus of the complex degree of coherence. The fully coherent case (single mode) is shown by the red dashed line. The two-mode contribution is shown by the black line.

The knowledge of the transverse coherence length of the LCLS beam and an estimate of its vertical focus size is sufficient to determine the degree of transverse coherence ζ_y in the vertical direction. We used the following definition of the total degree of transverse coherence [37]: $\zeta(\omega) = \int |W(\mathbf{r}_1, \mathbf{r}_2; \omega)|^2 d\mathbf{r}_1 d\mathbf{r}_2 [\int I(\mathbf{r}; \omega) d\mathbf{r}]^{-2}$, where $W(\mathbf{r}_1, \mathbf{r}_2; \omega)$ is the cross-spectral density (CSD) [35]. In the frame of the Gaussian Schell model [35,37], the total CSD $W(\mathbf{r}_1, \mathbf{r}_2; \omega)$ factorizes into the product of two independent components [38]: $W(\mathbf{r}_1, \mathbf{r}_2) = W(x_1, x_2) W(y_1, y_2)$. The same holds for the intensities $I(\mathbf{r}) = I(x) I(y)$. As a result, the total degree of transverse coherence can be presented as a product of the horizontal and vertical contributions $\zeta = \zeta_x \zeta_y$, where [37] $\zeta_{x,y} = (l_{x,y}^c/\sigma_{x,y}) \times [(l_{x,y}^c/\sigma_{x,y})^2 + 4]^{-1/2}$ and $l_{x,y}^c$ and $\sigma_{x,y}$ are the transverse coherence lengths and the beam sizes (rms), respectively. For the focused LCLS beam we determined $\zeta_y = 0.75 \pm 0.08$. A similar value ζ_x is expected in the horizontal direction, as the source size and the beam divergence at FEL sources have comparable magnitudes in both directions [25]. Thus the total degree of coherence for the full beam is $\zeta = 0.56 \pm 0.12$. This is comparable with the value obtained in simulations [20] for similar LCLS parameters.

The properties of highly coherent beams, such as XFEL beams, can also be conveniently described by their mode decomposition [35]. The CSD $W(y_1, y_2)$ can be decomposed into a sum of independent modes $W(y_1, y_2) = \sum_j \beta_j E_j^*(y_1) E_j(y_2)$, where β_j is the contribution of each mode $E_j(y)$. Applying the same Gaussian Schell model to the best shots in the vertical direction yields $\beta_1/\beta_0 = 0.14 \pm 0.05$ and $\beta_2/\beta_0 = 0.02 \pm 0.01$ for the first and for the second mode, respectively. This indicates that for separations of up to 15 μm, which corresponds to the FWHM of the beam, two modes are sufficient to describe the coherence properties of the beam in the vertical direction (see the inset in Fig. 3).

By using the mode decomposition of the CSD, the intensity in each direction (x, y) can be described by $I(x) = \sum_j \beta_j^x I_j(x)$, where $I_j(x)$ is the normalized intensity distribution of the jth mode. The total power of the wave field $P = \int I(x)I(y)dxdy$ is determined in this case by $P = P_0 + P_{0,1} + P_{1,0} + \cdots = \beta_0^x\beta_0^y + \beta_0^x\beta_1^y + \beta_1^x\beta_0^y + \cdots$, where we have neglected the contribution of modes higher than two. From this expression, the relative power of the dominant mode is $P_0/P = [1 + \beta_1^y/\beta_0^y + \beta_1^x/\beta_0^x]^{-1}$. Extrapolating our results to the horizontal direction, we estimate that $78 \pm 8\%$ of the total FEL beam power is concentrated in the dominant "TEM_{00}" mode. This value is substantially higher than at any existing x-ray source at that wavelength (it is about 1% for synchrotron sources [37]). From these results we conclude that at FEL sources such as LCLS almost the full photon flux can be used in coherence-based experiments, contrary to incoherent sources, where only a small fraction of the beam is available for such experiments.

By using the same model, the photon beam emittance ε_y in the vertical direction is given by [37] $\varepsilon_y = \sigma_y \cdot \sigma_y' = \lambda/(4\pi\zeta_y)$, where σ_y is the rms of the source size and σ_y' is the rms divergence of the photon beam. Substituting into this expression the measured value of the degree of transverse coherence ζ_y, we find that the emittance of the LCLS beam is $\varepsilon_y = 0.17 \pm 0.02$ nm rad. This agrees well with typical values reported for the LCLS photon beam at 800 eV with the source size $\sigma_y = 20$ μm and divergence $\sigma_y' = 8.5$ μrad [29]. For a diffraction-limited beam with $\zeta_y = 1$, the same source size and x-ray photon energy would have a smaller divergence of about 6.4 μrad (see Fig. 1 in Ref. [31]).

In conclusion, we have measured the coherence properties of the LCLS using the focused soft x-ray beam at a photon energy of 780 eV. The total degree of transverse coherence was found to be 56%, from which we estimate that 78% of the total power is contained in the dominant mode. Furthermore, the temporal coherence of the LCLS beam was measured to be 0.55 fs, in good agreement with an averaged LCLS spectrum at these energies. We foresee that this single-shot methodology for the coherence measurement of high-power, pulsed x-ray sources developed here can be extended to investigate the performance of the LCLS in different conditions of operation. Finally, understanding the high degree of coherence at XFEL sources—as demonstrated in this work—provides a solid foundation for future coherence-based experiments that exploit these bright, coherent x-ray beams.

Portions of this research were carried out on the SXR Instrument at the LCLS, a division of SLAC National Accelerator Laboratory and an Office of Science user facility operated by Stanford University for the U.S. Department of Energy. The SXR Instrument is funded by a consortium whose membership includes the LCLS, Stanford University through the Stanford Institute for Materials Energy Sciences (SIMES), Lawrence Berkeley National Laboratory (LBNL), University of Hamburg through the BMBF priority program FSP 301, and the Center for Free Electron Laser Science (CFEL). Part of the work was supported by BMBF Project No. 05K10CHG. Use of the Center for Nanoscale Materials was supported by the U. S. Department of Energy, Office of Science, Office of Basic Energy Sciences, under Contract No. DE-AC02-06CH11357. Part of this work was performed under the auspices of the U.S. Department of Energy by Lawrence Livermore National Laboratory under Contract No. DE-AC52-07NA27344. Financial support by the CNRS through the PEPS SASLELX program is acknowledged by J. L. We acknowledge a careful reading of the manuscript and suggestions made by Z. Huang and P. Emma.

*Corresponding author.
Ivan.Vartaniants@desy.de
†Provided the experimental realization.
Present address: European XFEL GmbH, Albert-Einstein-Ring 19, 22761 Hamburg, Germany.
Adrian.Mancuso@xfel.eu

[1] See Nature Milestones: Photons supplement (2010), http://www.nature.com/milestones/photons.
[2] W. Ackermann *et al.*, Nat. Photon. **1**, 336 (2007).
[3] P. Emma *et al.*, Nat. Photon. **4**, 641 (2010).
[4] T. Tanaka and T. Shintake, http://www-xfel.spring8.or.jp/SCSSCDR.pdf.
[5] M. Altarelli *et al.*, http://xfel.desy.de/tdr/index_eng.html.
[6] R. Neutze *et al.*, Nature (London) **406**, 752 (2000).
[7] A. P. Mancuso *et al.*, J. Biotechnol. **149**, 229 (2010).

[8] I. A. Vartanyants *et al.*, J. Synchrotron Radiat. **14**, 453 (2007).
[9] L. Young *et al.*, Nature (London) **466**, 56 (2010).
[10] H. N. Chapman *et al.*, Nature (London) **470**, 73 (2011).
[11] M. M. Seibert *et al.*, Nature (London) **470**, 78 (2011).
[12] J. Miao *et al.*, Nature (London) **400**, 342 (1999).
[13] M. A. Pfeifer *et al.*, Nature (London) **442**, 63 (2006).
[14] H. N. Chapman *et al.*, Nature Phys. **2**, 839 (2006).
[15] S. Eisebitt *et al.*, Nature (London) **432**, 885 (2004).
[16] G. B. Stephenson *et al.*, Nature Mater. **8**, 702 (2009).
[17] D. Sayre, Acta Crystallogr. **5**, 843 (1952).
[18] J. R. Fienup, Appl. Opt. **21**, 2758 (1982).
[19] E. L. Saldin *et al.*, New J. Phys. **12**, 035010 (2010).
[20] Y. Ding *et al.*, *Proceedings of the FEL2010 Conference, Malmö, Sweden, 2010* (Lund University, Lund, Sweden, 2010), p. 151.
[21] J. W. Goodman, *Statistical Optics* (Wiley, New York, 1985).
[22] B. J. Thompson and E. Wolf, J. Opt. Soc. Am. **47**, 895 (1957).
[23] D. Paterson *et al.*, Opt. Commun. **195**, 79 (2001).
[24] R. A. Bartels *et al.*, Science **297**, 376 (2002).
[25] A. Singer *et al.*, Phys. Rev. Lett. **101**, 254801 (2008).
[26] I. A. Vartanyants *et al.*, J. Phys. B **43**, 194016 (2010).
[27] R. A. Bartels *et al.*, Opt. Lett. **27**, 707 (2002).
[28] R. A. Dilanian *et al.*, Opt. Lett. **33**, 2341 (2008).
[29] J. N. Galayda *et al.*, J. Opt. Soc. Am. **27**, B106 (2010).
[30] P. Heimann *et al.*, Rev. Sci. Instrum. **82**, 093104 (2011).
[31] See Supplemental Material at http://link.aps.org/supplemental/10.1103/PhysRevLett.107.144801 for the detailed description of the apertures, data analysis, focus size measurements, beam divergence, and the impact of the positional uncertainty on the effective degree of coherence.
[32] R. Soufli *et al.*, Proc. SPIE Int. Soc. Opt. Eng. **7077**, 707716 (2008).
[33] R. Soufli *et al.*, Appl. Opt. **47**, 4633 (2008).
[34] A. Barty *et al.*, Opt. Express **17**, 15 508 (2009).
[35] L. Mandel and E. Wolf, *Optical Coherence and Quantum Optics* (Cambridge University Press, Cambridge, England, 1995).
[36] The natural bandwidth of the LCLS radiation is less than 1% at soft x-ray energies. Equation (1) is obtained under the paraxial and far-field approximations. It is assumed that diffraction patterns from different pinholes completely overlap at the detector position. Expression (1) also assumes that the radiation is stationary. With the duration of the LCLS pulses, $T_0 = 300$ fs, being much longer than the estimated coherence time $\tau_c \approx 0.55$ fs ($T_0 \gg \tau_c$), one may safely use stationary conditions.
[37] I. A. Vartanyants and A. Singer, New J. Phys. **12**, 035004 (2010).
[38] For brevity, we omit ω from future equations.